VERY SLOW STRAIN RATE STRESS-STRAIN BEHAVIOR AND RESISTING STRESS FOR CREEP IN A NICKEL-BASE SUPERALLOY

R. R. Jensen
T. E. Howson
J. K. Tien

Henry Krumb School of Mines, Columbia University
New York, New York 10027

Tensile stress-strain behavior of Udimet-115 is studied over a large temperature range (ambient - 982°C) and down to 10^{-6} per second strain rates. The lower strain rate yield stress data and the stresses corresponding to stress-strain steady state are used to show the direct correspondence between stress-strain and creep behaviors.

INTRODUCTION

Many studies of creep in complex particle strengthened alloys have found unreasonably high values of the applied stress exponent n and the creep activation energy Q when the creep results are described by a power law relationship in which the creep rate is a function of the applied stress, for example, see Refs. 1-4. It is well established now that the high n and Q values can be reduced to more meaningful levels that reflect expected characteristics predicted by theories of glide or recovery controlled dislocation creep if the creep rate $\dot{\varepsilon}$ is described in terms of an effective stress (5-14),

$$\dot{\varepsilon} = A[(\sigma-\sigma_R)/E]^n \exp(-Q/RT) \qquad (1)$$

where $\dot{\varepsilon}$ is the steady state or minimum creep rate, A is a material constant, σ is the applied stress and σ_R is a resisting stress or summation of resisting stresses against dislocation motion in the very low or creep strain rate regime of behavior,

E is the Young's modulus, n_o is the effective stress exponent and RT is the thermal energy.

The concept of resisting stress against deformation is relatively straightforward in the case of low homologous temperature tensile deformation. The resisting stress in that case is the yield strength plus any increment in the flow stress due to work hardening. In time dependent thermally assisted creep deformation, the origin and role of resisting stresses is less well understood, but certainly, just as for low homologous temperature tensile deformation, the resisting stresses against deformation at creep temperatures can be directly obtained from measurements of yield stress and flow stress made in constant strain rate tests at creep strain rates and temperatures.

In this paper, constant low strain rate high temperature data obtained over a wide range of temperatures and strain rates for a nickel base superalloy will be presented. First, some aspects of the data will be described since, other than the classic work of Hopkins, Gell and Leverant (15) on the Martin Metals Trademark Alloy Mar M200, little work on the temperature and strain rate dependence of the deformation behavior of nickel base superalloys has been performed. Then one of the many applications of this data will be presented, a study of the relationship betweeen stress-strain behavior and creep. For this the data and the different components of the total resisting stress against creep that can be measured in constant strain rate tests are discussed and compared to data obtained in creep experiments. Finally, the resisting stress measurements that are obtained are contrasted to the less easily understood resisting stresses obtained by other techniques.

EXPERIMENTAL PROCEDURE

The alloy used in this study was the Special Metals Corporation Alloy Udimet-115 (very similar to the INCO Trademark Alloy Nimonic 115), a nickel-base superalloy containing 40-45 volume percent γ' and whose composition in weight percent is Ni-14.3Cr-13.2Co-3.3Mo-4.9Al-3.7Ti-0.15C-0.16B-0.04Zr. The heat treatment employed for this alloy was a solutionizing treatment of 1232°C (2250°F) for 24 hours, furnace cooling to 1000°C (1832°F), then air cooling, followed by a carbide aging treatment of 982°C (1800°F) for 96 hours and air cooling. The resulting microstructure consists of 400 μm grains, with discrete carbides pinning grain boundaries, and γ' precipi-

tates in three size regimes, Fig. 1. The tensile specimens have a gage length of 12.8 mm (0.5 in) and a gage diameter of 3.2 mm (0.125 in).

High temperature tensile stress-strain tests on Udimet-115 were performed in air, using an MTS computer controlled servohydraulic material testing system equipped with a high temperature furnace and a special low flow rate servovalve to permit reliable low strain rate tensile experiments. The specimen temperature was controlled to within $\pm 1^{o}C$ with a gradient of less than $2^{o}C$ along the specimen gage length. The load train was equipped with universal joints to minimize bending moments. All stress-strain tests were performed at a constant true strain rate $\dot{\varepsilon}$ which corresponds to an engineering strain rate $\dot{e}$ of $\dot{e}=\dot{\varepsilon}(1+e)$, where e is the engineering strain. Experiments were performed spanning the range of temperatures from 30 to $982^{o}C$ and the range of strain rate from 10^{-2} to 10^{-6} sec^{-1}. Stress strain data were automatically acquired at preset strain intervals and permanently recorded on floppy magnetic discs. To facilitate the analysis of the data, all experiments were curve fit, using 5th order polynomial splines which provide an accurate representation of the data and an analytic form which is easily manipulated.

RESULTS

Typical stress-strain curves are shown in Fig. 2 for several different combinations of strain rate and temperature. The essential features to be noticed are that the apparent Stage II work hardening behavior in curve A is an exception for this alloy rather than the rule and is seen only for ambient temperature tests. Curve B exhibits a work hardening rate θ that does not follow Stage II behavior, which is typical of the elevated temperature behavior of this alloy. Interestingly, θ is higher for curve B than for curve A, even though the test temperature for B is higher than that for A. This is solely attributable to the unusual temperature dependences of the flow stress of the γ' phase. Curves C and D are typical of the high temperature-low strain rate behavior. They show necking relatively early in the test followed by unstable deformation. Curve D in particular is notable in that it more graphically illustrates saturation behavior of the stress, i.e., the existence of a steady state.

In Fig. 3, the 0.2% yield stress σ_y is plotted as a function of temperature and strain rate. As other researchers

have found for nickel-base superalloys (15,17,18), there is little strain rate or temperature dependence of σ_y from room temperature to about 540°C. Above this temperature, the σ_y versus temperature curve for each strain rate exhibits a slight peak, the temperature position of which increases with strain rate. Above about 750°C, σ_y decreases precipitously with temperature, perhaps due first to softening and then to dissolution of the γ' as the temperature is increased.

Figure 4 shows typical elevated temperature work hardening behavior for this alloy. At 760°C, the initial work hardening rate remains high for a relatively large range of stress as opposed to the work hardening rate at 927°C which decreases from the beginning of the test. However, it should be noted that in each case the lower portion of the curve which represents essentially all of the stress-strain curve following yield decreases linearly with stress. These straight line portions define an exponential approach of stress to a saturation stress σ_s according to the equation (19), $\sigma = \sigma_s[1-\exp(-e/e_0)]$, where e is the true strain and e_0 is a material parameter.

DISCUSSION

Although stress saturation or the saturation level extrapolated from the stress-strain curves during a stress-strain test may represent a steady state quantity, it remains to be shown that this steady state corresponds to the "steady state" which occurs during creep. To test the validity of this correspondence the saturation stresses as a function of the applied strain rates for each test temperature are shown in Fig. 5, in a double logarithmic plot as is the manner in which steady state creep data are analyzed. If the equivalence between the steady states of both types of tests holds, then for the same temperature, creep data of applied stress and steady state creep rate and stress-strain data of applied strain rate and saturation stress should lie on the same curve. Several creep tests were performed at 760°C under both constant applied stress and load conditions, and steady state creep rate data from these tests are also plotted in Fig. 5. An example of these 760°C creep curves is shown in Fig. 6 for an applied stress of 630 MPa.

As can be seen on the 760°C curve in Fig. 5, the agreement between the creep data and stress-strain data is quite good. Therefore, in spite of the fact that the deformation histories of a creep test and a stress-strain test prior to

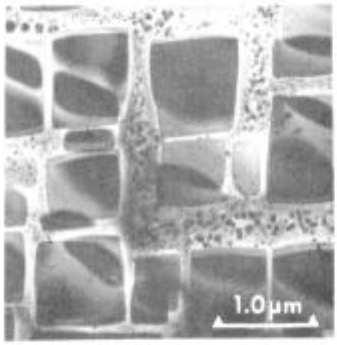

Fig. 1. TEM micrograph of Udimet 115 given two-stage heat treatment.

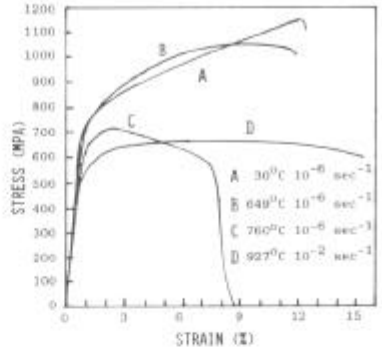

Fig. 2. Typical stress-strain curves for Udimet 115.

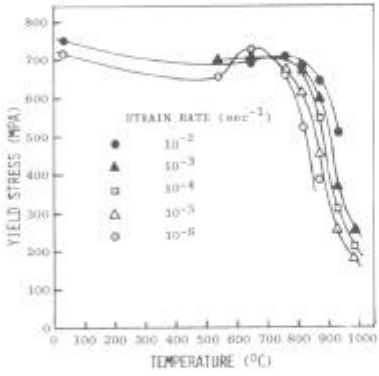

Fig. 3. 0.2% yield stress of Udimet 115 as a function of temperature and strain rate.

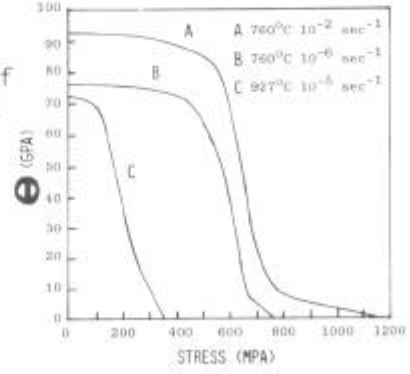

Fig. 4. Typical curves of work hardening rate as a function of stress for Udimet 115.

their respective steady states are different (i.e., creep is carried out at constant stress while the stress-strain test is carried out at constant strain rate), we believe that a stress-strain test during saturation is effectively equivalent to steady state creep of a strengthened alloy if the saturation stress and the applied stress are equal. The only difference between the two is that the dislocation substructure generated during primary creep of a creep test may be somewhat different from that produced during the work hardening stages of the stress-strain test. This would result in different values of the dislocation substructure component of the resisting stress, which may not be significant when compared with the particle strengthening component (see below) in superalloys. We are currently studying these substructures in the transmission electron microscope to determine if differences do exist.

The concept of effective stress for the rationalization of high temperature creep in particle strengthened materials, as introduced above, can now be utilized in the analysis of the stress-strain data obtained in this study. In simplest terms, the yield stress corresponds to the intrinsic resistance to dislocation motion due to solid solution elements and the strengthening second phase particles and any other dislocation obstacles. This is precisely what the resisting stress in Eq. (1) is envisioned to be. In Fig. 7, this concept has been applied to the data in Fig. 5, where now $\sigma_s-\sigma_y$ corresponds to the effective stress operating during steady state in a stress-strain test. The data for the 982°C and the 927°C tests are not included in Fig. 7 because these data are obtained in a temperature range where microstructural instabilities occur making analysis of the data difficult. The results in Fig. 7 show that the strain rate indeed obeys a power law relationship with respect to the effective stress $\sigma_s-\sigma_y$. The curvature exhibited by the 760°C curve and also slightly in the 815°C curve shows the well-known transition to power law breakdown behavior that occurs as the effective stress is raised. The effective stress exponent is between 4 and 5 for the curves in Fig. 7.

For comparison, some of the results of a study of creep in several particle strengthened nickel base alloys are shown in Fig. 8 (14). Minimum creep rates at 760°C are plotted as a function of an effective stress operating druing creep $\sigma-\sigma_p$, where σ_p is an applied stress independent component of σ_R due to the strengthening particles which were obtained by a curve fitting procedure (14). Here the effective stress exponent is four. Other researchers have also obtained an effective

stress exponent of about 4 when creep results of particle strengthened alloys are described in terms of an effective stress (8-12).

It is interesting that the value of σ_p for the same Udimet-115 alloy determined from creep tests (20) at about 10^{-8} per second creep rates lies close to the extrapolated 760°C curve of σ_y versus strain rate as determined by the stress-strain tests, Fig. 9. This extrapolation was done by assuming that the 760°C curve follows in parallel the 816°C curve. Finally, we note that the results of this study imply that dislocation creep of Udimet-115 is a recovery controlled process. It has been shown (Fig. 5) that creep data of applied stress and steady state creep rate and stress-strain data of applied strain rate and saturation stress lie on the same curve. During creep of Udimet-115, the total resisting stress against creep is equal to the applied stress.

Accordingly, in this study a different method for measurement of resisting stresses in creep has been presented. By measuring yield stresses and saturation stresses in constant strain rate tests carried out at creep strain rates and temperatures, the creep resisting stress due to the matrix plus strengthening second phase particles, and that due to dislocations can be identified.

Other measurements of creep resisting stresses have usually been made in stress change experiments, but the exact physical significance of these measurements is not easily understood, especially in the case of microstructurally complex alloys.

In the strain-transient or stress transient test (6,7), when the strain rate or stress in a creep or constant strain rate test reaches a steady state the stress is quickly reduced and the subsequent positive or negative rate of change of strain or stress is carefully measured. The resisting stress in these experiments, termed the average internal stress, corresponds to the critical reduced stress after the stress drop at which initially the rate of change of stress or strain is zero. Internal stress measurements have been made on a variety of pure metals and solid solution alloys. The internal stress is thought to represent the long range dislocation back stress characteristic of the substructure developed at the initial applied stress before the stress drop. It has been pointed out, however, that anelastic processes contribute to the strain rate immediately after the stress drop (21), and this complicates interpretation of the internal stress. In

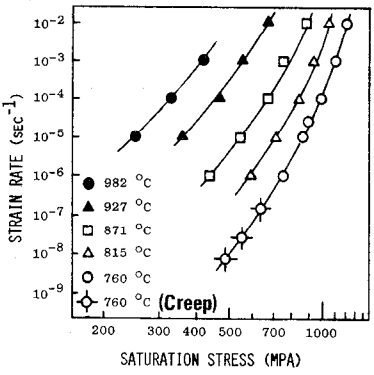

Fig. 5. Saturation stress vs strain rate and temperature with 760° C creep data (⊕).

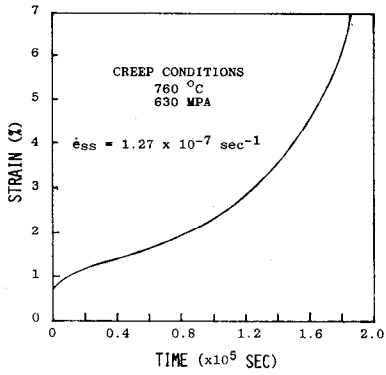

Fig. 6. Typical creep curve for Udimet 115.

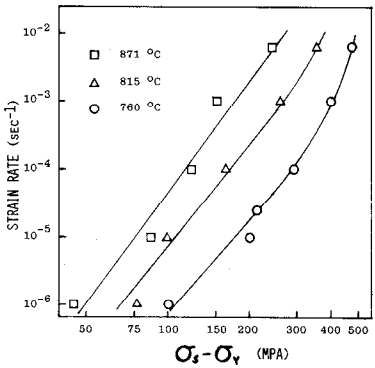

Fig. 7. Strain rate vs effective stress in constant strain rate experiments.

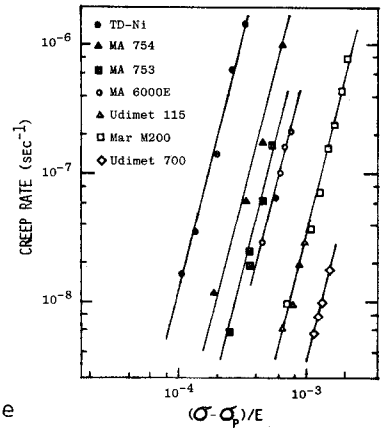

Fig. 8. Creep rate vs normalized effective stress for several particle strengthened systems.

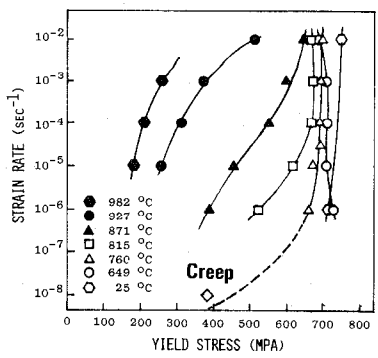

Fig. 9. 0.2% yield stress as a function of strain rate and temperature with extrapolation for 760° C and 10^{-8} sec^{-1} strain rate creep σ_p for 760° C creep (◇).

these types of experiments, there are also the problems associated with measurements of strain at extremely low strain rates.

A different method for measuring resisting stresses in creep involves repeated small stress-dips (8,9,11). After the initial stress drop, an incubation period of zero creep rate is observed. As soon as the dealy time ends and creep recommences at the reduced stress level, a second small stress decrease is made, followed by a longer incubation period, etc. From a plot of the cumulative incubation period $\Sigma\Delta t$ against the cumulative stress reduction $\Sigma\Delta\sigma$ a resisting stress, termed a friction stress σ_0, is defined as the stress remaining on the specimen when the cumulative incubation period appears infinite, i.e., $\sigma_0=\sigma-\Sigma\Delta\sigma$. Measurements of friction stress have been made on, and have been used to, rationalize the creep behavior of many pure metals, solid solution alloys and multiphase precipitation or dispersion strengthened materials.

Measurements of friction stress have been criticized (22) because of the possible inaccuracy in determining the asymptotic value of cumulative stress reduction when the cumulative incubation period appears infinite. There is with this method also the problem of measuring strain at very small strain rates. In addition, this test may not result in a realistic value for the net resisting stress, especially in the heavily alloyed nickel-base superalloys where the solid solution component may be significant and also strain rate dependent.

The complexity of the situation is further illustrated by the fact that two fundamentally different kinds of behavior are reported in stress change experiments. Researchers who measure friction stresses report incubation periods of zero creep after small reductions of the applied stress, while groups that measure internal stresses report no incubation periods after stress drops.

In view of these problems, we feel that measuring or extrapolating for resisting stresses by performing low constant strain rate, high temperature experiments may be potentially of value. In conclusion, it should be pointed out that the at temperature and at strain rate flow stress values can be directly input into structural design. Currently, we are continuing the stress-strain effort to include tests into compression which may result in the separation of solid solution component, particle component and true back stress components. These latter components may be of interest in understanding cyclic creep and fatigue of superalloys (23).

ACKNOWLEDGEMENT

We gratefully acknowledge the National Science Foundation for supporting this research under grant NSF-DMR77-11281.

REFERENCES

1. B.A. Wilcox and A.H. Clauer, Trans. TMS-AIME 236, 570 (1966).
2. J.S. Benjamin and R.L. Cairns, Modern Devel. in Powder Metall. 5, 47 (1970).
3. F.T. Furillo, J.M. Davidson, L.A. Jackman and J.K. Tien, Mater. Sci. Eng. 39, 267 (1979).
4. K. Aning and J.K. Tien, "Creep and Stress Rupture Behavior of a Wrought Nickel Base Superalloy in Air and Vacuum," Mater. Sci. Eng. 1979, in press.
5. W.D. Nix and C.R. Barrett, Trans. ASM 61, 695 (1968).
6. C.N. Alquist and W.D. Nix, Acta Met. 19, 373 (1971).
7. M. Pahutova and J. Cadek, Mater. Sci. Eng. 11, 151 (1973).
8. K.R. Williams and B. Wilshire, Met. Sci. J. 7, 176 (1973).
9. J.D. Parker and B. Wilshire, Met. Sci. J. 9, 248 (1975).
10. R. Lagneborg and B. Bergman, Met. Sci. 10, 20 (1976).
11. W.J. Evans and G.F. Harrison, Met. Sci. 10, 307 (1976).
12. R.W. Lund and W.D. Nix, Acta Met. 24, 469 (1976).
13. S. Purushothaman and J.K. Tien, Acta Met. 26, 519 (1978).
14. O. Ajaja, T.E. Howson, S. Purushothaman and J.K. Tien, "Role of Alloy Matrix in the Creep Behavior of Particle Strengthened Alloys," accepted for publication in Mater. Sci. Eng., 1980.
15. G.R. Leverant, M. Gell and S.W. Hopkins, Mater. Sci. Eng. 8, 125 (1971).
16. P.H. Thornton, R.G. Davies and T.L. Johnston, Met. Trans. 1, 207 (1970).
17. S.M. Copley and B.H. Kear, Trans. AIME 239, 984 (1967).
18. S.M. Copley, B.H. Kear and G.M. Rowe, Mater. Sci. Eng. 10, 87 (1972).
19. U.F. Kocks, J. Eng. Mats. Technol. 98, 76 (1976).
20. J.M. Davidson, Eng. Sc. D. Thesis, Columbia University, New York (1978).
21. G.J. Lloyd and R.J. McElroy, Acta Met. 22, 339 (1974).
22. G.C. Gibeling and W.D. Nix, Met. Sci. 11, 453 (1977).
23. D. Matejczyk and J.K. Tien, unpublished research, Columbia University, (1980).